Research on the application potential of spent biological activated carbon from BAC process to remove radionuclides Sr^{2+} from water

Lihua Dong[1] · Chengliang Wu[1] · Yingjie Han[1] · Shujie Pan[1] · Zhansheng Wang[2] · Guanghui Zhang[1] · Li'an Hou[1,3] · Ping Gu[1]

Abstract

The spent biological activated carbon (SBAC) as solid waste is used to study the removal of radioactive Sr^{2+} in water. The results show that SBAC adsorbs Sr^{2+} reaching equilibrium within 3 min and the adsorption is an exothermic reaction. The removal rate can reach more than 85%, desorption rate is less than 6.16%, and it can also achieve 40% removal in river water. The three-round regeneration efficiencies are all ~ 100%. The adsorption process is without secondary pollution. SBAC has good potential for the removal of radioactive Sr^{2+} in water.

Keywords Strontium adsorption in water · Activated carbon · Regeneration · Secondary pollution · Practical application

Introduction

With the development of the nuclear industry, radioactive waste is produced in large quantities, and the discharge of radioactive waste is an important source of radionuclides entering the environment. Among them, radioactive strontium (^{90}Sr) has a half-life of 28.8 years and a large share of radioactivity, which is the main nuclides in radioactive water. It is a kind of osteogenic β-radiation source [1, 2]. The biochemical properties similar to calcium will make it participate in the metabolic process. It is difficult to excrete after ingestion, leading to white blood cells, red blood cells and platelets are significantly reduced, regenerative disorders occur, and even lead to leukemia or osteosarcoma [3, 4]. Therefore, the removal of ^{90}Sr has been receiving widespread attention.

To date, techniques for removing radioactive strontium (Sr^{2+}) from aqueous solutions include adsorption, chemical precipitation, membrane separation, and solvent extraction [5–9] etc. Among them, the chemical precipitation method may introduce a large number of salts, and some extractants in the extraction method are highly toxic and the membrane separation method has a low yield [5]. Therefore, the technical choice of treating radioactive containing Sr^{2+} is increasingly inclined to adsorption. Many researchers have tested the removal of Sr^{2+} by a variety of organic and inorganic adsorbents, including diatomaceous earth [10], goethite [11], hematite [12], bentonite [13], kaolinite [14], montmorillonite [15], clay minerals [16], pecan shells [17], zeolites [18] and activated carbon (AC), as well as some new adsorbents [19] etc. Although, due to high surface area, porous structure and functional group, AC has been the most popular and widely used adsorbent in water treatment technology all over the world and is used to remove a broad spectrum of impurities from water [20], there are few studies on the adsorption of Sr^{2+} by AC, and the effect is not satisfactory. Shawabkeh et al. (2002) showed that the removal rate of AC to Sr^{2+} was 56.3% when the AC dosage was 1 g L^{-1} [17]. The AC used by Chegrouche et al. (2009) had a removal rate of 60% after 8 h of adsorption under optimal conditions [21]. Moloukhia et al. (2016) modified the coconut shell charcoal to adsorb a variety of radioactive elements, and the adsorption of Sr^{2+} was less than 40% under the condition of 10 g L^{-1} dosage and 4 h contact time [22]. Studies by Caccin et al. (2013) and

✉ Lihua Dong
donglihua12@tsinghua.org.cn

1 School of Environmental Science and Engineering, Tianjin University, Tianjin 300072, China

2 School of Environment, Tsinghua University, Beijing 100084, China

3 Xi'an High-Tech Institute, Xi'an 710025, China

Kubota et al. (2013) have even shown that the ACs they used is difficult to remove Sr^{2+} [23, 24].

As can be seen that the effect of AC on Sr^{2+} removal is not ideal, but Andersson et al. (2001) pointed out in the research that the granular activated carbon (GAC) used in the BAC process for a certain period of time adsorbed a large amount of calcium, aluminum, and a certain amount of iron, copper, and cadmium [25]. This proves that some changes have taken place in GAC during the BAC process. Will these changes bring new peculiar properties to AC? Dong et al. (2018, 2020) confirmed that the spent biological activated carbon (SBAC) from BAC process can adsorb metal ions lead and cadmium with the maximum removal rate of > 90% [20, 26]. Moreover, SBACs irrespective of using-time presented stable adsorption abilities (> 99%) for Pb^{2+} (2.0–8.0 mg L^{-1}) with the maximum uptake of 168.07 mg g^{-1}, and their adsorption mechanism for Pb(II) were confirmed, including the dominant ion exchange (H^+, Ca^{2+} etc.) and metal complexation with hydroxyl and carboxyl functional groups [26]. This confirms the ability of SBAC to adsorb metal ions. On this basis, this work use SBAC to study the removal and application of Sr^{2+} in water. Undoubtedly, this will not only help to find a new low-cost adsorbent for the possible radioactive Sr^{2+} pollution, but also make the widely used BAC advanced feedwater treatment process safer in case of sudden radioactive contamination, that is, the BAC process has the ability to deal with radioactive strontium pollution.

Using stable isotope of Sr, which has similar chemical property as radioactive strontium (^{90}Sr) [27], the potential of SBAC for the removal of radionuclides Sr^{2+} were studied in this paper. SBACs with different using-time were sampled from the same drinking water treatment plant with our previous study [20, 26]. The main objectives of this study are: (1) to characterize the adsorption of Sr^{2+} by SBAC, (2) to study the adsorption properties of Sr^{2+} from the perspectives of kinetics, isotherms, thermodynamics and other influencing factors, (3) to study the adsorption mechanism, (4) to test the applicability of SBAC to Sr^{2+} adsorption.

Experimental

The SBAC samples taken from a certain drinking water treat plant (used 5, 6 and 7 years) called SBAC-5, SBAC-6, SBAC-7, were naturally dried. Then the samples were ground to a powder until 95% of the SBAC particles passed through a 325-mesh sieve, and then dried at 80 °C for 3 h in a vacuum drying oven. The Sr^{2+} water solution was prepared by dissolving strontium chloride hexahydrate ([nat]Sr, $SrCl_2 \cdot 6H_2O$, 99%, Tianjin Guangfu Fine Research Institute, China) in pure water (Elix 10, 15.0 MΩ cm at 298 K). Sodium hydroxide (NaOH, AR, Tianjin No. 3 Chemical

Reagent Factory, China), Hydrochloric acid, Nitric acid (HCl, AR, HNO_3, AR, Tianjin Damao Chemical Reagent Factory, China), Calcium chloride dihydrate, Magnesium chloride dihydrate ($CaCl_2 \cdot 2H_2O$, AR, $MgCl_2 \cdot 2H_2O$, AR, Tianjin KeMiou Chemical Reagent Co., Ltd., China), Cesium chloride ([133]Cs, CsCl, 99%, Tianjin Guangfu Fine Research Institute, China) were used in this work.

The concentrations of Sr^{2+} and other metal ions were determined by ICP-OES (iCAP™ 7400, Thermo Electron Corporation, USA). The pH value was measured using a portable multimeter equipped with a pH probe (HQ40D, Hach). Fourier transform infrared (FTIR) spectroscopy was performed on a NEXUS 870 pectrophotometer using the KBr disk method (IRAffinity-1S). X-ray photoelectron spectroscopy (XPS) (Thermo Scientific ESCALAB 250 spectrometer) determined the elemental composition and chemical bonding state of the SBACs sample. All binding energy values were corrected from adventitious hydrocarbon to the C 1s line at 284.8 eV.

According to ASTM D3860-98 (2014) [28] standards, the adsorption experiments were respectively conducted as follows.

The precisely weighed adsorbent (SBAC) was mixed with a certain initial concentration of Sr^{2+} solution in a centrifuge tube. Considering possible water pollution incidents, drinking water quality requirements and detection limit of ICP-OES, the initial concentration of Sr^{2+} was set to approximately 5 mg L^{-1}. The centrifuge tube containing the mixture was placed in a thermostatic shaker (HT-2102C, Herrytech) and shaken at a specific temperature. When the adsorption equilibrium was reached, the adsorbent was immediately filtered through 0.45 μm filter to remove the SBAC. The filtrate was acidulated using 1% HNO_3 before the concentration of Sr^{2+} was determined by ICP-OES. All cases were duplicated under the identical conditions and the results recorded as average values.

The amount of Sr^{2+} adsorbed on SBAC (q_e, mg g^{-1}) [29], adsorption efficiency (Ads, %) [19] and distribution coefficient (K_d, mL g^{-1}) [30, 31] were respectively calculated by the following equations:

$$q_e = V \frac{C_o - C_e}{m} \tag{1}$$

$$\text{Ads} = 100 \frac{C_o - C_e}{C_o} \tag{2}$$

$$K_d = \frac{V}{m} \times \frac{C_o - C_e}{C_e} \tag{3}$$

where C_o (mg L^{-1}) and C_e (mg L^{-1}) are the initial and equilibrium concentrations of Sr^{2+} in aqueous solutions,

respectively, m (g) is the mass of the adsorbent, and V (L) is the aqueous volume.

The adsorption isotherm, thermodynamics and kinetics were studied according to the method of Sr^{2+} batch adsorption experiments.

The kinetic equations, isothermal models and thermodynamic study used to fit the adsorption experiment data are shown in Table 1.

The influence factors on Sr^{2+} adsorption were investigated according to the batch models including dosage of SBACs (0–8 g L^{-1}), the initial concentration of Sr^{2+}(5–100 mg L^{-1}), the pH of the solution (2.6–11, 0.1 M HNO_3 or 0.1 M NaOH was added to the solution), the temperature of adsorption (283–313 K), coexisting cations (dissolving $CaCl_2·2H_2O$ and $MgCl_2·2H_2O$ in Sr^{2+} solution, total concentration of Ca^{2+} and Mg^{2+} is in the range of 0–200 mg L^{-1}).

Results and discussion

Adsorption kinetics

To study the kinetics of Sr^{2+} adsorption, 2.00 g L^{-1} of the adsorbent was added into 5.78 mg L^{-1} Sr^{2+} solution at 298 K and the remaining Sr^{2+} concentration was tested at various contact times (0, 1, 3, 5, 10, 20, 45, 60 min). The results were shown in Fig. 1a and Table 2. The dosage of the adsorbent was set to 2 g L^{-1}, which is completely sufficient when the initial concentration of Sr^{2+} is 5.78 mg L^{-1} as shown at "Adsorption capacity" section.

Figure 1 shows the adsorption kinetic curves of Sr^{2+} on SBAC-5, SBAC-6 and SBAC-7. It can be seen from Fig. 1a that the concentration of Sr^{2+} in the solution drops rapidly in the first few minutes of the adsorption process, and Ads of Sr^{2+} reaches 85% in almost 3 min. As the adsorption time continues to increase, Ads of Sr^{2+} does not change much, only increases to about 86.6%. This shows that the reaction between Sr^{2+} and SBAC is instantaneous and exhibits the characteristics of a chemical reaction.

The pseudo first order, the pseudo second order and intraparticle diffusion models were used to fit the kinetics of Sr^{2+} adsorption, respectively. The results are shown in Fig. 1b–d. It can be seen from Fig. 1 and Table 2 that the adsorption kinetics of Sr^{2+} by SBAC-5, SBAC-6, and SBAC-7 completely conform to the pseudo second order, and the R^2 value of the linear fit all reaches 1. It can be seen from the kinetic analysis that SBAC reaches equilibrium very quickly during the adsorption of Sr^{2+}, and Ads reaches 85%, which is very beneficial for practical applications.

Adsorption isotherms and thermodynamics

The adsorption isotherms and thermodynamic study were tested at 283, 298 and 313 K by changing the initial concentration of Sr^{2+} (5.0–200 mg L^{-1}). And thermodynamic calculations were performed based on the above results.

Langmuir isotherm, Freundlich isotherm and Dubinin–Radushkevich (D–R) isotherm were respectively used to fit the inter action between SBAC and Sr^{2+}. The fitting results show that the adsorption isotherms of SBAC-5, SBAC-6 and SBAC-7 are more consistent with the Langmuir

Table 1 The equations of kinetic, isotherm models and thermodynamic study [3, 19, 26, 32, 33]

	Models	Equation	Nomenclature
Adsorption isotherms	Langmuir	$\frac{C_e}{q_e} = \frac{1}{K_L q_m} + \frac{C_e}{q_m}$	C_e: equilibrium concentration, mg L^{-1}
	Freundlich	$\ln q_e = \ln K_f + \frac{1}{n} \ln C_e$	K_L: Langmuir adsorption equilibrium constant, L mg^{-1}
	Dubinin–Radushkevich (D–R)	$\ln(q_e) = \ln(q_s) - K_{ad} \cdot \varepsilon^2$	q_m: the maximum metal uptake, mg g^{-1}
		$\varepsilon = RT\ln(1 + 1/C_e)$	K_f: constant relating the adsorption capacity, L g^{-1}
			n: Freundlich constants
			q_s: theoretical saturation capacity, mg g^{-1}
Kinetics studies	Pseudo first order	$\ln(q_e - q_t) = \ln q_e - K_1 t$	K_{ad}: adsorption equilibrium constant
	Pseudo second order	$t/q_t = (1/K_2 q_e^2) + (1/q_e)t$	ε: Polanyi potential
	Intraparticle diffusion	$q_t = K_I d_t^{0.5} + C$	R: gas constant, 8.314 J mol^{-1} K^{-1})
			T: absolute temperature, K
Thermodynamic		$\ln K_C = -\Delta G^\Theta/RT$	q_e: amount adsorbate equilibrium, mg g^{-1}
		$\ln K_C = (\Delta S^\Theta/R) - (\Delta H^\Theta/RT)$	q_t: amount adsorbate retained at time, mg g^{-1}
		(the van't Hoff equation)	t: time, min
		$\Delta G^\Theta = \Delta H^\Theta - T\Delta S^\Theta$	K_1: Pseudo first order rate constant, min^{-1}
			K_2: Pseudo second order rate constant, g mg^{-1} min^{-1}
			K_I: Intraparticle diffusion rate constant, mg g^{-1} $min^{-0.5}$
			C: thickness of the boundary layer, mg g^{-1}
			K_C: adsorption equilibrium constant, mg^{-1}
			ΔG^Θ: free energy, kJ mol^{-1}
			ΔH^Θ: change in enthalpy, kJ mol^{-1}
			ΔS^Θ: change in entropy, J mol^{-1} K^{-1}

Fig. 1 SBACs' kinetic models for Sr^{2+} ($C_o = 5.78$ mg L^{-1}, $W/V = 2.0$ g L^{-1}, $T = 298$ K, pH $= 6.1$, $t = 0$–60 min)
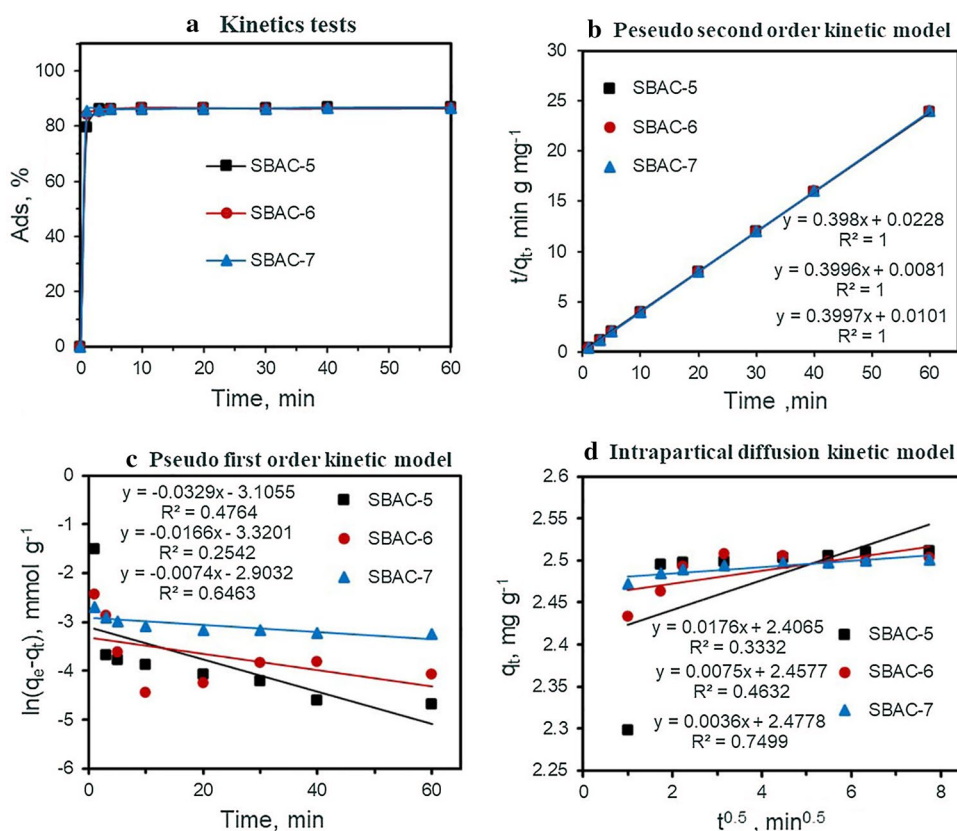

Table 2 Parameters of the kinetics model for Sr^{2+} adsorption on SBAC

Model	Experimental value	The pseudo first order			The pseudo second order			The intraparticle diffusion		
Parameter	q_e (mg g^{-1})	K_1 (min^{-1})	q_e (mg g^{-1})	R_1^2	K_2 (g mg^{-1} min^{-1})	q_e (mg g^{-1})	R_2^2	C	K_I (mg g^{-1} min$^{-0.5}$)	R^2
SBAC-5	2.52	0.07576	0.0448	0.4764	6.9475	2.5125	1	2.4065	0.0176	0.3332
SBAC-6	2.52	0.03822	0.03614	0.2542	19.7136	2.5025	1	2.4577	0.0075	0.4258
SBAC-7	2.54	0.01704	0.05484	0.6463	15.8178	2.5018	1	2.4778	0.0036	0.7499

model, as shown in Fig. 2a–c, the correlation coefficient R^2 is greater 0.976, indicating that Sr^{2+} had monolayer adsorption on the surface of SBAC. As can be obtained from Table 3 the maximum saturated adsorption capacity of SABC-7 is 30.98 mg g^{-1}, followed by SBAC-6, was 30.41 mg g^{-1}, SBAC-5 was 29.33 mg g^{-1} at room temperature of 298 K. Considering the practical application, the reaction temperature selected in this paper is 298 K (room temperature).

As seen from Fig. 2d that the curve of $\ln K_C$ versus $1/T$ of the van't Hoff equations is a linear equation with a higher regression coefficient, and R^2 values of SBACs are 0.9765, 0.8574, and 0.9509, respectively. Therefore, the thermodynamic parameters can be obtained based on the above results, and the calculation results are listed in Table 3. It can be seen from Table 3 that the adsorption capacity q_m of SBAC decreases with increasing temperature, indicating

that low temperature is more conducive to the adsorption of Sr^{2+} by SBAC, which is consistent with the logical relationship between the thermodynamic parameter ΔH^Θ and a negative value. In addition, the ΔG^Θ is negative value, indicating that the adsorption of Sr^{2+} on SBACs is a spontaneous process. The ΔH^Θ is negative, indicating that the adsorption process is exothermic, so the lower temperature is beneficial to adsorption.

Comparison of Sr^{2+} adsorption with other AC adsorbents

Table 4 shows the comparison of Sr^{2+} adsorption with other adsorbents. It can be seen from Table 4 that compared with the other AC adsorbents, Ads of SBAC is the highest.
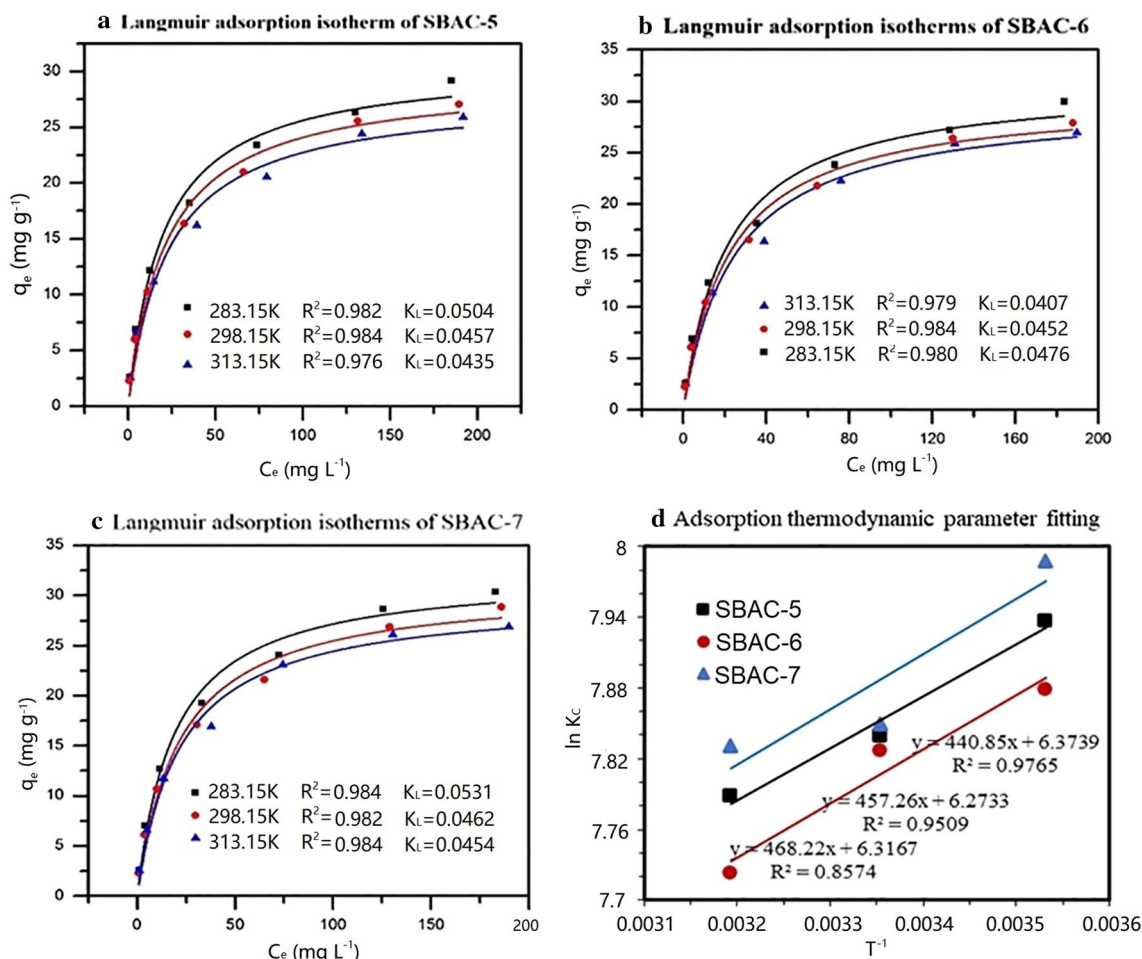
Fig. 2 Langmuir adsorption isotherms and adsorption thermodynamic parameter fitting of Sr^{2+} to SBACs ($C_o = 5$–200 mg L^{-1}, $W/V = 2$ g L^{-1}, pH $= 6.0$, $t = 120$ min)

Table 3 SBACs' isothermal and thermodynamic parameters of Sr^{2+}

Model		Experiment q_e(max)	Langmuir model			Thermodynamic			
Material	T (K)		K_L (L mg^{-1})	q_m (mg g^{-1})	R^2	R^2	$\Delta H^\ominus$ (KJ mol^{-1})	$\Delta S^\ominus$ (J mol^{-1})	$\Delta G^\ominus$ (KJ mol^{-1})
SBAC-5	283	29.15	0.05044	30.6633	0.982	0.977	− 3.665	52.995	− 18.686
	298	27.05	0.04573	29.3295	0.984				− 19.433
	313	25.90	0.04348	27.9487	0.976				− 20.279
SBAC-6	283	30.00	0.04757	31.8090	0.980	0.951	− 3.802	52.159	− 18.548
	298	27.90	0.04519	30.4151	0.984				− 19.403
	313	26.95	0.04071	29.9455	0.979				− 20.108
SBAC-7	283	30.35	0.05307	32.2764	0.984	0.857	− 3.893	52.520	− 18.806
	298	28.85	0.04622	30.9843	0.982				− 19.459
	313	26.90	0.04538	29.8113	0.984				− 20.390

Influence factors on Sr^{2+} adsorption

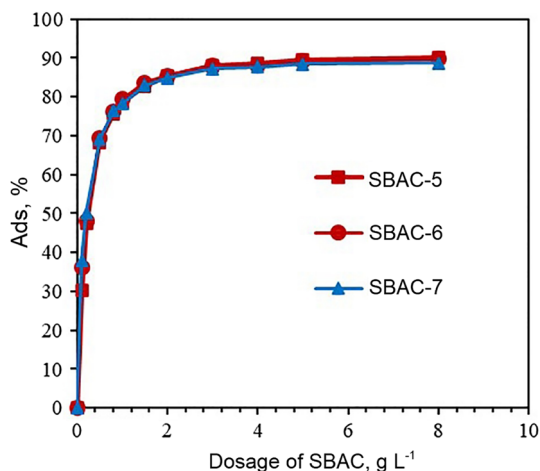### Adsorption capacity

Figure 3 shows the effect of SBAC dosage (0–8 g L^{-1}) on

the removal of Sr^{2+}. As can be seen from Fig. 3, when the initial concentration of the Sr^{2+} solution is 5 mg L^{-1}, with the increase of the dosage of SBAC from 0 to 2 g L^{-1}, the Ads of Sr^{2+} by SBAC with different service years rapidly increased to more than 85%. With the further increase of

Table 4 The comparison between this work and other adsorbents

Materials	Dosage (g L^{-1})	C_o (g L^{-1})	T (K)	pH	Ads (%)	References
The granular activated carbon supplied by Merck, Germany	–	0.1	293.15	4.0	56.3	[34]
Modified activated carbon (by oxidation using H$_2$O$_2$ and HNO$_3$)	10.0	0.8	298 ± 1	1.73–6.35	< 40	[22]
Coconut-activated carbon	1.25–25	0.096	Room temperature	Natural	Close to 0	[24]
A commercial activated carbon obtained by physical activation of coconut shell	20–100 mg	0.01, 0.03	296.15	Natural	Close to 0	[23]
SBAC-5	2	0.0050	298	6.1	> 85	This work
SBAC-6					> 85	
SBAC-7					> 85	

Fig. 3 Effect of SBACs' dosage on Sr^{2+} adsorption (C_o = 5 mg L^{-1}, W/V = 0–8 g L^{-1}, T = 298 K, pH = 6.1, t = 120 min)

SBAC dosage from 2 to 8 g L^{-1}, the Ads of Sr^{2+} increased slowly to 89% and reach equilibrium. Therefore, the dosage of adsorbent in this work was chosen to be 2.0 g L^{-1}.

It can be seen that there is a big breakthrough comparing with Ads of 16% of the virgin AC at dosage of 2 g L^{-1} and initial concentration of 5 mg L^{-1} (Fig. 4a). It should

be attributed to be the changes of the surface functional groups and the increasing of metal ions absorbed in AC during BAC process ("Adsorption mechanism" section and Supplementary information). The results of FT-IR and XPS show that compared with virgin AC, SBAC has more oxygen-containing functional groups and calcium and magnesium content on its surface (Fig. S4, Tab. S2). It proves that SBAC from the BAC process did have the potential of removing Sr^{2+} from water.

Then the effects of different initial Sr^{2+} concentrations (5–100 mg L^{-1}) were investigated, while keeping other conditions unchanged.

It can be seen from Fig. 4 that when the dosage of adsorbent is 2 g L^{-1}, Ads gradually decreased with the increase of the initial concentration due to insufficient SBAC dosages. That is, when the concentration of Sr^{2+} in the water to be treated is high, it is necessary to increase the dosage of SBAC to achieve the desired adsorption effect.

The affinity of the material for Sr^{2+} can be described by K_d. Compared to other AC adsorbents, such as, the modified activated carbon (by oxidation using H$_2$O$_2$ and HNO$_3$) [22] showed K_d values of 63.08 ml g^{-1} at pH = 5.6, activated carbon A-14 [35] showed K_d values of 10 mL g^{-1}. As shown in Fig. 4b, SBAC material had a high affinity

Fig. 4 Effect of initial concentration on Sr^{2+} adsorption (**a**: Ads changing with the increase of the initial concentration, **b**: K_d changing with the increase of the initial concentration) (C_o = 5–100 mg L^{-1}, W/V = 2.0 g L^{-1}, T = 298 K, pH = 6.1, t = 120 min)
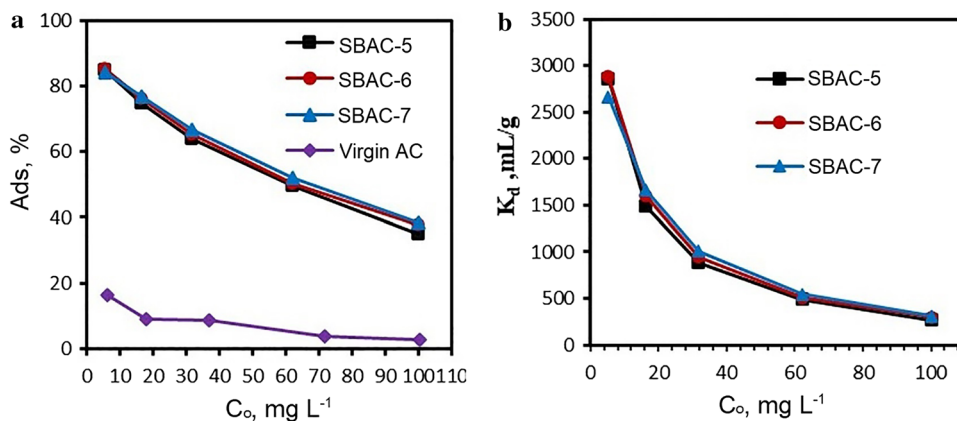
for Sr^{2+}, particularly at low Sr^{2+} concentrations, the values of K_d were higher than 10^3 mL g^{-1} within the C_o range of 5–15 mg L^{-1}.

Moreover, the desorption experiments of SBAC after adsorption of Sr^{2+} samples (SBAC-Sr) also prove the strong adsorption capacity of SBAC for Sr^{2+}, which were performed by adding SBAC-Sr (2 g L^{-1}) in pure water (pH ~ 6.1, 298 K) and shaking for 12 h. The desorption rates of Sr^{2+} are shown in Table 5. It can be seen that SBACs released a very small portion of loaded Sr^{2+} (4.43%, 6.16%, 3.90%) into water, implying that Sr^{2+} was firmly bound on SBACs. Therefore, in terms of the desorption after adsorption is concerned, the amount of Sr^{2+} adsorbed by SBAC is much higher than the amount of desorption.

Based on the above adsorption test and desorption test, it can be concluded that SBAC has a great advantage over virgin AC in ability to adsorb Sr^{2+}. At the same time, according to the desorption test, it can be seen that the adsorption of SBACs on Sr^{2+} is stable.

Effect of pH on Sr^{2+} adsorption

Since the pH of the radioactive water may be extremely acidic or alkaline, it is necessary to study the effect of pH on the adsorption of Sr^{2+}. The effect of the initial pH on the removal efficiency of Sr^{2+} by SBACs is presented in Fig. 5. Six different pH were tested (2.44, 4.14, 8.20, 10.12, 10.95 and 11.70). It can be seen from Fig. 5 that when the pH at about 2.0, Ads of Sr^{2+} is very low for all SBACs. With the increase of pH from 4.0 to more than 11.0, Ads is significantly increased and increased to 99.9%. This should be attributed to that the isoelectric point of SBAC is less than 4.14 (SBAC-5, SBAC-6, SBAC-7 all less than 2.86, [26]). Under extremely acidic conditions, the surface of SBAC is protonated because of the high concentration of H^+, which causes a strong positive charge on the surface of SBAC, thereby preventing the adsorption of Sr^{2+} by SBAC due to electrostatic repulsion. When the pH of the solution is higher than the isoelectric point of SBAC, the surface of SBAC is negatively charged, which helps SBAC to adsorb positively charged metal ions, such as Sr^{2+}. Therefore, in addition to the strong acid environment, SBAC is negatively charged in

Fig. 5 Effect of pH on Sr^{2+} adsorption ($C_o = 5.454$ mg L^{-1}, $W/V = 2.0$ g L^{-1}, $T = 298$ K, pH $= 2.6$–11, $t = 120$ min)

the aqueous solution, which provides a strong basic condition for SBAC to adsorb metal ions.

Effect of coexisting ions on Sr^{2+} adsorption

Since Ca^{2+} and Mg^{2+} are widely present in actual waters, coexisting ions solution are prepared using $CaCl_2 \cdot 2H_2O$ and $MgCl_2 \cdot 2H_2O$. Ca^{2+} and Mg^{2+} with concentrations ranging from 0 to 200 mg L^{-1} (0 mg L^{-1}, 50 mg L^{-1}, 100 mg L^{-1}, 150 mg L^{-1}, and 200 mg L^{-1}) was added to approximately 5.0 mg L^{-1} Sr^{2+} solution. Adsorption experiments of SABC-5, SABC-6 and SABC-7 on Sr^{2+} were respectively carried out in above coexisting solutions, and the results are shown in Fig. 6.

It can be seen that compared with the absence of coexisting ions, Ads of Sr^{2+} by SABC-5, SABC-6 and SABC-7 decreased significantly with the increase of Ca^{2+} and Mg^{2+}
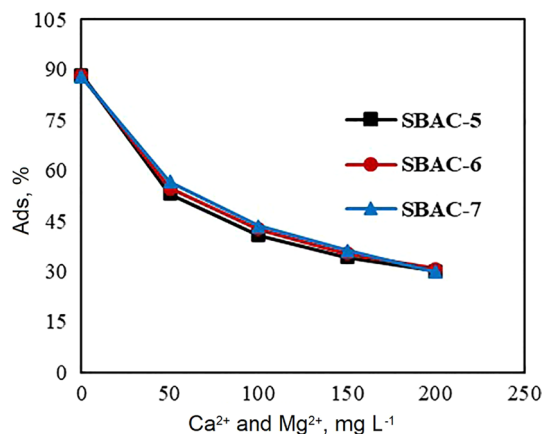
Table 5 Desorption of Sr^{2+} on SBAC

Sample	Adsorption capacity (mg g^{-1})	Desorption capacity (mg g^{-1})	Desorption rate (%)
SBAC-5-Sr	2.293	0.102	4.43
SBAC-6-Sr	2.257	0.139	6.16
SBAC-7-Sr	2.260	0.088	3.90

Fig. 6 Effect of coexisting ions on Sr^{2+} adsorption ($C_o = 5$ mg L^{-1}, $W/V = 2.0$ g L^{-1}, $T = 298$ K, pH $= 6.1$, $t = 120$ min)

ions, decreasing from 88% to about 30%. It should be attributed to the competition of Sr^{2+}, Ca^{2+} and Mg^{2+} for the same adsorption active sites, which verifies that Sr^{2+} has the similar biochemical properties with Ca^{2+} [3]. Undoubtedly, if Sr^{2+} enters the drinking water system, it will endanger human health even cause serious illness like leukemia or osteosarcoma [3].

Adsorption mechanism

FT-IR surface functional group analysis before and after adsorption of Sr^{2+}

A Fourier infrared spectrometer was used to analyze the changes of the surface functional groups of SBAC-5, SBAC-6, and SBAC-7 before and after the adsorption of Sr^{2+}.

It can be seen from Fig. S1 that SBAC-5, SBAC-6 and SBAC-7 have two round and blunt strong peaks at 3433 cm^{-1} and 3190 cm^{-1}, respectively. They are caused by O–H stretching vibration of carboxyl group and phenolic hydroxyl group [25]. The peak intensity at 3190 cm^{-1} decreases significantly after Sr^{2+} adsorption, probably because the OH of the carboxyl group and phenolic hydroxyl group is consumed in the adsorption reaction. The peak at 1125 cm^{-1} may be C–O stretching vibration [25], which disappears obviously after adsorbing Sr^{2+}, probably because the alcohol is reacted. Different from the adsorption of Pb^{2+} [26], the asymmetric tensile vibration of the carboxylate in the range of 1565–1665 cm^{-1} [36] produced insignificant changes in absorption peaks.

XPS analysis before and after adsorption of strontium

The XPS analysis of SBACs before and after the adsorption of Sr^{2+} as shown in Table S1 indicates that, after SBAC adsorbed Sr^{2+}, O and Sr content increased, Ca content decreased. The increase of O indicates that it participated in the reaction. The mechanism analysis is shown in the supplementary material.

As for the decrease of Ca content, it is speculated that during the adsorption of Sr^{2+} by SBAC, other metal ions (like Ca^{2+}, etc.) that had been adsorbed on the surface of SBAC were released into the solution through the exchange mechanism, Sr^{2+} is adsorbed on the surface of SBAC, so release of Ca^{2+}, etc. was tested after SBAC adsorbed Sr^{2+} ("Release of other metal ions" section).

Release of other metal ions

Desorption of Ca^{2+}, Mg^{2+} and Al^{3+} were tested in Sr^{2+} solution. The results are shown at Fig. S3. Linear slopes between the amount of Sr^{2+} adsorbed and the amount of desorbed Ca^{2+} are 0.717, 0.759, and 0.692 for SBAC-5, SBAC-6

and SBAC-7. For Mg^{2+}, the slopes are between 0.05 and 0.1, all R^2 were greater than 0.98. It can be concluded that approximately 75% to 85% of Sr^{2+} adsorbed is indeed due to exchange with Ca^{2+} (70% to 75%) and Mg^{2+} (5% to 10%).

From the above analysis, the mechanism of SBAC removing Sr^{2+} from aqueous solution is mainly composed of the following two parts similar to another work [26]: (1) ion exchange, mainly the exchange of Sr^{2+} and Ca^{2+}, (2) the complexation of oxygen-containing functional groups on the carbon surface with metal Sr^{2+}, mainly hydroxyl.

Regeneration of SBAC after Sr^{2+} adsorption

In order to explore the reuse potential of SBAC after adsorbing Sr^{2+} and the recoverability of the adsorbed Sr^{2+}, taking SBAC-7 as an example, a 0.1 M HCl solution was used to regenerate SBAC-Sr. The detailed experimental process is as follows: First, SBAC-Sr is regenerated with 0.1 M HCl solution. Afterwards, the regenerated SABC sample is rinsed with pure water until there is no significant change in pH. The sample is dried in the vacuum drying oven and continues to be used for adsorbing Sr^{2+}. The experiment was repeated three times, and the test results are shown in Table 6.

As can be seen from Table 6, the adsorption capacity of SBAC for Sr^{2+} have gradually increased as the number of regenerations increases. It's speculated that as result of the action of HCl, the metal ions previously adsorbed on the SBAC are released, providing more adsorption sites. The above results show that the adsorption capacity of SBAC after three-round repeated regeneration can complete recovery and even increase.

Possible secondary pollution analysis of SBAC

When SBAC is used to remove metal ions in actual water, it is necessary to consider whether SBAC itself as waste is hazardous when used in actual water. That is if other substances will release, causing secondary pollution to the water body. Therefore, the possible releases of organic matter and metal ions in SBAC were studied in this section.

Table 6 Desorption and regeneration of SBAC after Sr^{2+} adsorption

SBAC-7	Capacity of Sr^{2+} (mg g^{-1})	Regeneration efficiency (%)
Virgin adsorption	2.336	–
After 1st regeneration	2.796	119.69
After 2nd regeneration	2.820	100.86
After 3rd regeneration	2.820	100.00

Release of organic matter in SBAC

Considering that SBACs are the saturated AC used in the BAC process without pretreatment, the organic pollutants adsorbed on it may have a certain negative impact on its reuse. Therefore, release experiments of organic matter were respectively conducted in pure water, tap water, and actual river water (taken from the river water in the Pei-yangn campus district of Tianjin University). The main ionic water quality indicators in different water bodies are shown in Table 7.

The release experiment measured changes in organic carbon (NPOC) by TOC-L CPN (Shimadzu, Co. LTD, detection limit is 0.010 mg L^{-1}) through the same experimental method with Sr^{2+} batch adsorption experiments under the condition of SBAC content of 0.20 g L^{-1}. The experiment lasted a total of 1320 min, and samples were taken at 60 min, 480 min and 1320 min respectively. The results are shown in Table 8.

From the data in Table 8, it can be seen that for different water bodies, there is a clear difference in the release of organic matter in SBAC, among which the release in laboratory pure water is more obvious, followed by the tap water, and the least in river water. That is, when SBAC is used for the removal of metals in actual water, the effect of organic matter release is negligible. However, the necessary pre-experiments must be carried out before application to rule out the possible comprehensive effects.

Judging from the release results of the three SBACs with different service years, the release value did not change much, and there was no obvious difference. As far as the release time is concerned, the results of 60 min, 480 min and 1320 min are also not significantly different, that is, the release of organic matter adsorbed by SBAC will not change significantly with the extension of use time.

Release of metal ions in SBAC

SBAC (0.20 g L^{-1}, 2.0 g L^{-1}) was added in 50 ml of pure water. After shaking for 12 h, the supernatant was taken to detect the concentration of metal ions, and the release was investigated. The results are shown in Table 9, which indicated the detected metal ions are mainly Ca^{2+}, Mg^{2+}, Al^{3+}, and no release of harmful metals was detected.

Table 7 Main metal ions in test water

Concentration (mg L^{-1})	K^+	Na^+	Ca^{2+}	Mg^{2+}	Al^{3+}
Pure water	ND^a	ND^a	ND^a	ND^a	ND^a
Tap water	3.60	21.76	36.30	12.32	0.128
Campus river	14.73	211.8	32.45	44.85	0.16

^{a}Not detected

Table 8 Release of NPOC on SBAC

Background water	AC samples (0.20 g L^{-1})	Release NPOC value (mg L^{-1})		
		60 min	480 min	1320 min
Pure water	–	1.109	1.109	1.109
	SBAC-5	4.793	6.830	6.630
	SBAC-6	4.459	7.887	4.876
	SBAC-7	5.500	8.725	6.863
Tap water	–	25.68	25.68	25.68
	SBAC-5	31.00	33.76	32.52
	SBAC-6	31.32	31.46	30.68
	SBAC-7	31.02	32.77	34.58
Campus river	–	50.42	50.42	50.42
	SBAC-5	52.42	52.38	48.97
	SBAC-6	54.36	52.83	51.30
	SBAC-7	55.12	57.27	50.73

Considering that the concentrations of Ca^{2+}, Mg^{2+}, and Al^{3+} in tap water are 36.30, 13.05, and 0.128 mg L^{-1}; the concentrations of Ca^{2+}, Mg^{2+}, and Al^{3+} in river water are 32.45, 44.85, and 0.16 mg L^{-1} (as shown in Table 9), the concentration is extremely small compared to its background concentration in actual water, which is within an acceptable range. In addition, when SBAC is used in actual water, because it is rich in cations, which will inhibit the release of metal ions, therefore, the amount of release is less than that in pure water. In summary, the release of metal in SBAC will not affect its application in actual water.

The foregoing analysis of release test can prove that when SBAC is used for the adsorption and removal of Sr^{2+} in actual water, the organic matter released by SBAC itself can be ignored; the metal released by itself is non-harmful metal and the content is small. In summary, the release of organic matter and metal ions adsorbed on the surface of SBAC shows that SBAC is feasible for the removal of heavy metals and radionuclides in actual water in terms of safety and secondary pollution.

Table 9 Release of metal ions on SBAC

Dosage of SBAC (g L^{-1})	Activated carbon samples	Release concentration value (mg L^{-1})		
		Ca^{2+}	Mg^{2+}	Al^{3+}
0.2	SBAC-5	0.5888	0.0983	0.0184
	SBAC-6	0.8677	0.0647	0.0169
	SBAC-7	0.7650	0.1150	0.0339
2.0	SBAC-5	3.089	0.5444	0.0317
	SBAC-6	3.731	0.3225	0.0353
	SBAC-7	4.046	0.7996	0.0409

Application of SBAC adsorption of Sr^{2+} in river water

The solution containing Sr^{2+} was prepared with river water ("Release of organic matter in SBAC" section) to simulate the actual water body contaminated with Sr^{2+}. The sampled river water was first filtered through a 0.22 μm filter membrane to remove suspended solids and green algae before use. Using the same method as the previous adsorption isotherm experiment, the adsorption capacity of SBAC to Sr^{2+} in river water was investigated.

It can be seen from Fig. 7 that, compared with Ads in pure water, SBAC-5, SBAC-6 and SBAC-7 have a certain degree of reduction in Ads of Sr^{2+} in real river water. The maximum Ads of Sr^{2+} decreased from about 85% in pure water to 34–40% in river water. This can be explained by the aforementioned adsorption mechanism. The large amount of Ca^{2+}, Mg^{2+} and other cations in the river affect the
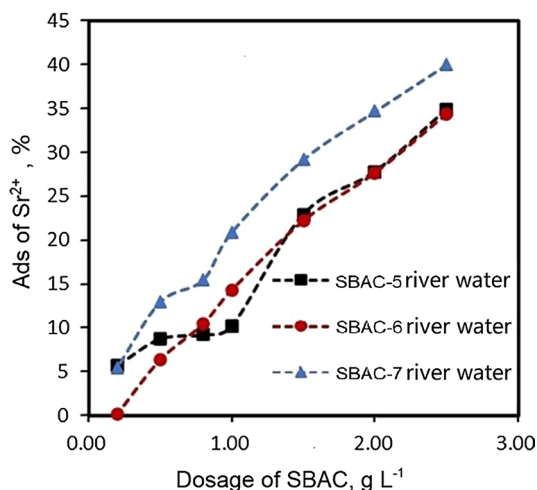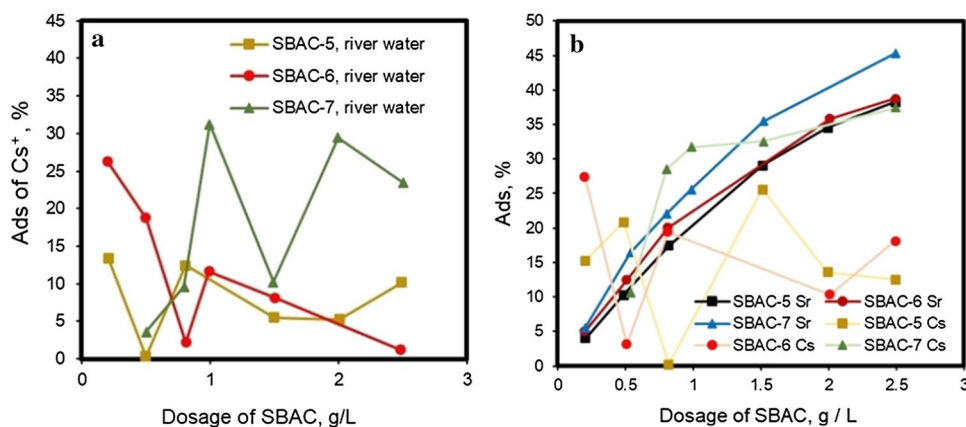
adsorption of SBAC. In addition, the large amount of organic matter in the river water (NPOC value of 50.42 mg L^{-1}) may also affect ability to adsorb metal ions of SBAC [26]. Nevertheless, compared with other AC adsorbents from Table 4, SBAC still shows the best removal effect in actual river water. In addition, SBAC has nearly zero cost and does not require any pretreatment, achieving direct reuse of resources.

Considering that ^{90}Sr and ^{137}Cs usually occur simultaneously in radioactive wastewater [37–39], the adsorption effect of SBAC for Cs^+, and the coexistence experiment of Sr^{2+} and Cs^+ in river water are tested. It can be seen from Fig. 8a that the adsorption of Cs^+ in river water is not regular and worse than Sr^{2+}, which may be related to the different ionic radius and element properties of Sr^{2+} and Cs^+. At the same time, the complex internal conditions of river water may affect the adsorption effect of Cs^+, and the specific reasons need to be further explored. It is worth noting that the coexistence experiment of Sr^{2+} and Cs^+ shows that when they coexist in river water, the removal rate of Sr^{2+} by SBAC is not affected by Cs^+ (Fig. 8b). Therefore, when SBAC is applied to the treatment of wastewater containing Sr^{2+} and Cs^+, other methods should be considered to remove Cs^+.

Conclusions

In this work, three SBACs were investigated on removal of Sr^{2+} from water. There are somethings that draw people attention.

The adsorption of Sr^{2+} by SBAC has fast speed, high removal rate far above virgin AC, which shows the potential of SBAC for the removal of Sr^{2+}. The removal mechanism of Sr^{2+} mainly has the following two points: Sr^{2+} exchanges with Ca^{2+} from SBAC and complexation of oxygen-containing functional groups on the surface (mainly hydroxyl groups and lactone group).

The leaching test shows the application of SBAC in water is safe. The regeneration experiment of SBACs shows their

Fig. 7 SBAC adsorbs Sr^{2+} in river water ($C_o = 5.199$ mg L^{-1}, $W/V = 0$–2.5 g L^{-1}, $T = 298$ K, pH $= 9.10$, $t = 120$ min)

Fig. 8 SBAC adsorbs Cs^+(**a**), Sr^{2+} and Cs^+(**b**) in river water ($C_o(Cs^+) = 6.7$ mg L^{-1}, $C_o(Sr^{2+}) = 5.7$ mg L^{-1}, $W/V = 0$–2.5 g L^{-1}, $T = 298$ K, pH $= 9.1$, $t = 120$ min)

excellent regeneration performance. The desorption of SBACs shows that the amount of Sr^{2+} adsorbed by SBAC is much higher than the amount of desorption. The above verifications indicate the feasibility of SBAC being used in actual water. More importantly, SBAC has the advantages of low price, and good adsorption and regeneration performance. In short, the work has good practical application value.

References

1. Castrillejo M, Casacuberta N, Breier CF, Pike SM, Masqué P, Buesseler KO (2016) Reassessment of 90Sr, 137Cs, and 134Cs in the coast off Japan derived from the Fukushima Dai-ichi nuclear accident. Environ Sci Technol 50(1):173–180. https://doi.org/10.1021/acs.est.5b03903

2. Attallah MF, Rizk SE, Shady SA (2018) Separation of 152 + 154Eu, 90Sr from radioactive waste effluent using liquid–liquid extraction by polyglycerol phthalate. Nucl Sci Tech 29(6):84. https://doi.org/10.1007/s41365-018-0423-z

3. Ghandhi SA, Weber W, Melo D, Doyle-Eisele M, Chowdhury M, Guilmette R, Amundson SA (2015) Effect of 90Sr internal emitter on gene expression in mouse blood. BMC Genom. https://doi.org/10.1186/s12864-015-1774-z

4. Zhang Z, Gu P, Zhang M, Yan S, Dong L, Zhang G (2019) Synthesis of a robust layered metal sulfide for rapid and effective removal of Sr2 + from aqueous solutions. Chem Eng J 372:1205–1215. https://doi.org/10.1016/j.cej.2019.04.193

5. Wu L, Zhang G, Wang Q, La Hou GuP (2014) Removal of strontium from liquid waste using a hydraulic pellet co-precipitation microfiltration (HPC-MF) process. Desalination 349:31–38. https://doi.org/10.1016/j.desal.2014.06.020

6. Zhang L, Lu Y, Liu Y-L, Li M, Zhao H-Y, Hou L-A (2016) High flux MWCNTs-interlinked GO hybrid membranes survived in cross-flow filtration for the treatment of strontium-containing wastewater. J Hazard Mater 320:187–193. https://doi.org/10.1016/j.jhazmat.2016.08.020

7. Deli D, Law K, Liu Z, Crouch DJ, Livens FR, Yeates SG (2012) Selective removal of 90Sr and 60Co from aqueous solution using N-aza-crown ether functional poly(NIPAM) hydrogels. React Funct Polym 72(6):414–419. https://doi.org/10.1016/j.reactfunctpolym.2012.03.013

8. Wen T, Zhao Z, Shen C, Li J, Tan X, Zeb A, Wang X, Xu AW (2016) Multifunctional flexible free-standing titanate nanobelt membranes as efficient sorbents for the removal of radioactive (90)Sr(2 +) and (137)Cs(+) ions and oils. Sci Rep 6:20920. https://doi.org/10.1038/srep20920

9. Attallah MF, Borai EH, Hilal MA, Shehata FA, Abo-Aly MM (2011) Utilization of different crown ethers impregnated polymeric resin for treatment of low level liquid radioactive waste by column chromatography. J Hazard Mater 195:73–81. https://doi.org/10.1016/j.jhazmat.2011.08.007

10. Huang C-P, Lin T-Y, Chiao L-H, Chen H-B (2012) Characterization of radioactive contaminants and water treatment trials for the Taiwan Research Reactor's spent fuel pool. J Hazard Mater 233–234:140–147. https://doi.org/10.1016/j.jhazmat.2012.07.009

11. Sahai N, Carroll SA, Roberts S, O'Day PA (2000) X-ray absorption spectroscopy of strontium(II) coordination: II. Sorption and precipitation at kaolinite, amorphous silica, and goethite surfaces. J Colloid Interface Sci 222(2):198–212. https://doi.org/10.1006/jcis.1999.6562

12. Karasyova ON, Ivanova LI, Lakshtanov LZ, Lövgren L (1999) Strontium sorption on hematite at elevated temperatures. J Colloid Interface Sci 220(2):419–428. https://doi.org/10.1006/jcis.1999.6474

13. Liang T-J, Hsu C-N, Liou D-C (1993) Modified Freundlich sorption of cesium and strontium on Wyoming bentonite. Appl Radiat Isot 44(9):1205–1208. https://doi.org/10.1016/0969-8043(93)90065-I

14. Jeong CH (2001) Mineralogical and hydrochemical effects on adsorption removal of cesium-137 and strontium-90 by kaolinite. J Environ Sci Health Part A Toxic Hazard Subst Environ Eng 6(36):1089–1099

15. Papachristodoulou CA, Assimakopoulos PA, Gangas NHJ (2002) Strontium adsorption properties of an aluminum-pillared montmorillonite carrying carboxylate functional groups. J Colloid Interface Sci 245(1):32–39. https://doi.org/10.1006/jcis.2001.7988

16. Cole T, Bidoglio G, Soupioni M, O'Gorman M, Gibson N (2000) Diffusion mechanisms of multiple strontium species in clay. Geochim Cosmochim Acta 64(3):385–396. https://doi.org/10.1016/S0016-7037(99)00324-5

17. Shawabkeh RA, Rockstraw DA, Bhada RK (2002) Copper and strontium adsorption by a novel carbon material manufactured from pecan shells. Carbon 40(5):781–786. https://doi.org/10.1016/S0008-6223(01)00198-1

18. Al-Jubouri SM, Curry NA, Holmes SM (2016) Hierarchical porous structured zeolite composite for removal of ionic contaminants from waste streams and effective encapsulation of hazardous waste. J Hazard Mater 320:241–251. https://doi.org/10.1016/j.jhazmat.2016.08.011

19. Zhang M, Gu P, Zhang Z, Liu J, Dong L, Zhang G (2018) Effective, rapid and selective adsorption of radioactive Sr2 + from aqueous solution by a novel metal sulfide adsorbent. Chem Eng J 351:668–677. https://doi.org/10.1016/j.cej.2018.06.069

20. Dong L, Hou L, Wang Z, Gu P, Chen G, Jiang R (2018) A new function of spent activated carbon in BAC process: removing heavy metals by ion exchange mechanism. J Hazard Mater 359(OCT.5):76–84

21. Chegrouche S, Mellah A, Barkat M (2009) Removal of strontium from aqueous solutions by adsorption onto activated carbon: kinetic and thermodynamic studies. Desalination 235(1):306–318. https://doi.org/10.1016/j.desal.2008.01.018

22. Moloukhia H, Hegazy WS, Abdel-Galil EA, Mahrous SS (2016) Removal of Eu3 +, Ce3 +, Sr2 +, and Cs + ions from radioactive waste solutions by modified activated carbon prepared from coconut shells. Chem Ecol 32(4):324–345. https://doi.org/10.1080/02757540.2016.1139089

23. Caccin M, Giacobbo F, Da Ros M, Besozzi L, Mariani M (2013) Adsorption of uranium, cesium and strontium onto coconut shell activated carbon. J Radioanal Nucl Chem 297(1):9–18. https://doi.org/10.1007/s10967-012-2305-x

24. Kubota T, Fukutani S, Ohta T, Mahara Y (2013) Removal of radioactive cesium, strontium, and iodine from natural waters using bentonite, zeolite, and activated carbon. J Radioanal Nucl Chem 296(2):981–984. https://doi.org/10.1007/s10967-012-2068-4

25. Andersson A, Laurent P, Kihn A, Prévost M, Servais P (2001) Impact of temperature on nitrification in biological activated carbon (BAC) filters used for drinking water treatment. Water Res 35(12):2923–2934

26. Dong L, Pan S, Liu J, Wang Z, La Hou, Chen G (2020) Performance and mechanism of Pb(II) removal from water by the spent biological activated carbon (SBAC) with different using-time. J Water Process Eng. https://doi.org/10.1016/j.jwpe.2020.101255

27. Sato I, Kudo H, Tsuda S (2011) Removal efficiency of water purifier and adsorbent for iodine, cesium, strontium, barium and zirconium in drinking water. J Toxicol Sci 36(6):829–834

28. International ASoTM (2014) Standard practice for determination of adsorptive capacity of activated carbon by aqueous phase isotherm technique, vol ASTM D3860-98. West Conshohocken, PA. https://doi.org/10.1520/d3860-98r14

29. Attallah MF, Borai EH, Allan KF (2009) Kinetic and thermodynamic studies for cesium removal from low-level liquid radioactive waste using impregnated polymeric material. Radiochemistry 51(6):622–627. https://doi.org/10.1134/s1066362209060113

30. Attallah MF, Abd-Elhamid AI, Ahmed IM, Aly HF (2018) Possible use of synthesized nano silica functionalized by Prussian blue as sorbent for removal of certain radionuclides from liquid radioactive waste. J Mol Liq 261:379–386. https://doi.org/10.1016/j.molliq.2018.04.050

31. Nayl AA, Ahmed IM, Abd-Elhamid AI, Aly HF, Attallah MF (2020) Selective sorption of 134Cs and 60Co radioisotopes using synthetic nanocopper ferrocyanide-SiO2 materials. Sep Purif Technol. https://doi.org/10.1016/j.seppur.2019.116060

32. Rizk HE, Attallah MF, Ali AMI (2017) Investigations on sorption performance of some radionuclides, heavy metals and lanthanides using mesoporous adsorbent material. J Radioanal Nucl Chem 314(3):2475–2487. https://doi.org/10.1007/s10967-017-5620-4

33. Attallah MF, Allan KF, Mahmoud MR (2015) Synthesis of poly(acrylic acid–maleic acid)SiO2/Al2O3 as novel composite material for cesium removal from acidic solutions. J Radioanal Nucl Chem 307(2):1231–1241. https://doi.org/10.1007/s10967-015-4349-1

34. Chegrouche S, Mellah A, Barkat M (2009) Removal of strontium from aqueous solutions by adsorption onto activated carbon: kinetic and thermodynamic studies. Desalination 235:306–318

35. Alarifi A, Hanafi H (2010) Adsorption of cesium, thallium, strontium and cobalt radionuclides using activated carbon. J At Mol Sci. https://doi.org/10.4208/jams.100809.112309a

36. Ganesh I, Sekhar PSC, Padmanabham G, Sundararajan G (2012) Influence of Li-doping on structural characteristics and photocatalytic activity of ZnO nano-powder formed in a novel solution pyro-hydrolysis route. Appl Surf Sci 259:524–537. https://doi.org/10.1016/j.apsusc.2012.07.077

37. Attallah MF, Hassan HS, Youssef MA (2019) Synthesis and sorption potential study of Al2O3ZrO2CeO2 composite material for removal of some radionuclides from radioactive waste effluent. Appl Radiat Isot 147:40–47. https://doi.org/10.1016/j.apradiso.2019.01.015

38. Hamed MM, Attallah MF, Metwally SS (2014) Simultaneous solid phase extraction of cobalt, strontium and cesium from liquid radioactive waste using microcrystalline naphthalene. Radiochim Acta. https://doi.org/10.1515/ract-2013-2200

39. Borai EH, Hilal MA, Attallah MF, Shehata FA (2008) Improvement of radioactive liquid waste treatment efficiency by sequential cationic and anionic ion exchangers. Radiochim Acta 96(7):441–447. https://doi.org/10.1524/ract.2008.1506